



Supplement of

Analysis of secondary organic aerosol simulation bias in the Community Earth System Model (CESM2.1)

Yaman Liu et al.

Correspondence to: Xinyi Dong (dongxy@nju.edu.cn)

The copyright of individual parts of the supplement might differ from the article licence.

Table S1. 15 reactions^a relative to SOAG production.

	Reactants	Products	Rate Constant
1	ISOP + OH	ISOP + OH + 0.0031*SOAG0 + 0.0035*SOAG1 + 0.0003*SOAG2 + 0.0271*SOAG3 + 0.0474*SOAG4	2.54e-11 exp(410/T)
2	ISOP + O3	ISOP + O3 + 0.0033*SOAG3	1.05e-14 exp(-2000/T)
3	ISOP + NO3	ISOP + NO3 + 0.059024*SOAG3 + 0.025024*SOAG4	3.03e-12 exp(-446/T)
4	MTERP + NO3	MTERP + NO3 + 0.17493*SOAG3 + 0.59019*SOAG4	1.20e-12 exp(490/T)
5	MTERP + O3	MTERP + O3 + 0.0508*SOAG0 + 0.1149*SOAG1 + 0.0348*SOAG2 + 0.0554*SOAG3 + 0.1278*SOAG4	6.30e-16 exp(-580/T)
6	MTERP + OH	MTERP + OH + 0.0508*SOAG0 + 0.1149*SOAG1 + 0.0348*SOAG2 + 0.0554*SOAG3 + 0.1278*SOAG4	1.20e-11 exp(440/T)
7	BCARY + NO3	BCARY + NO3 + 0.17493*SOAG3 + 0.59019*SOAG4	1.900e-11
8	BCARY + O3	BCARY + O3 + 0.2202*SOAG0 + 0.2067*SOAG1 + 0.0653*SOAG2 + 0.1284*SOAG3 + 0.114*SOAG4	1.200e-14
9	BCARY + OH	BCARY + OH + 0.2202*SOAG0 + 0.2067*SOAG1 + 0.0653*SOAG2 + 0.1284*SOAG3 + 0.114*SOAG4	2.000e-10
10	BENZENE + OH	BENZENE + OH + 0.0023*SOAG0 + 0.0008*SOAG1 + 0.0843*SOAG2 + 0.0443*SOAG3 + 0.1621*SOAG4	2.30e-12 exp(-193/T)
11	TOLUENE + OH	TOLUENE + OH + 0.1364*SOAG0 + 0.0101*SOAG1 + 0.0763*SOAG2 + 0.2157*SOAG3 + 0.0232*SOAG4	1.70e-12 exp(352/T)
12	XYLENES + OH	XYLENES + OH + 0.1677*SOAG0 + 0.0174*SOAG1 + 0.086*SOAG2 + 0.0512*SOAG3 + 0.1598*SOAG4	1.700e-11
13	IVOC + OH	OH + 0.2381*SOAG0 + 0.1308*SOAG1 + 0.0348*SOAG2 + 0.0076*SOAG3 + 0.0113*SOAG4	1.340e-11
14	SVOC + OH	OH + 0.5931*SOAG0 + 0.1534*SOAG1 + 0.0459*SOAG2 + 0.0085*SOAG3 + 0.0128*SOAG4	1.340e-11
15	GLYOXAL + aer	SOAG0	f(SAD), $\gamma=0.0002^b$

^a Emmons et al. (2020)

^b Function of aerosol surface area density (SAD), see Emmons et al. (2020) for details

Table S2. Chemical formula and description of species in Table S1(Emmons et al., 2020).

Species	Chemical Formula	Description
ISOP	C5H8	isoprene
MTERP	C10H16	lumped monoterpenes
BCARY	C15H24	beta-caryophyllene and other sesquiterpenes
BENZENE	C6H6	benzene
TOLUENE	C7H8	toluene
XYLENES	C8H10	lumped xylenes
IVOC	C13H28	intermediate volatility organic precursor of VBS SOA
SVOC	C22H46	semi-volatile organic precursor of VBS SOA
GLYOXAL	C2H2O2	glyoxal
OH	OH	hydroxyl radical
O3	O3	ozone
NO3	NO3	nitrate radical
SOAG0	C15H38O2	SOA gas-phase precursor VBS bin 0 (mol.wt. = 250 g/mol) (Shrivastava et al., 2015)
SOAG1	C15H38O2	SOA gas-phase precursor VBS bin 1
SOAG2	C15H38O2	SOA gas-phase precursor VBS bin 2
SOAG3	C15H38O2	SOA gas-phase precursor VBS bin 3
SOAG4	C15H38O2	SOA gas-phase precursor VBS bin 4

Table S3. The average OA of four ATom campaigns (Wofsy et al., 2018) and CAM-Chem-SD; the mean bias (MB), normalized mean bias (NMB), normalized mean error (NME), root mean square error (RMSE) and correlation coefficient (CC) between campaigns and CAM-Chem-SD.

Aircraft	Mean Obs.	Mean Sim.	MB	NMB(%)	NME(%)	RMSE	CC
ATom1	0.38	0.26	-0.12	-29.6	64.1	0.70	0.72
ATom2	0.16	0.10	-0.06	-39.6	76.8	0.26	0.58
ATom3	0.28	0.13	-0.15	-54.7	76.5	0.61	0.40
ATom4	0.38	0.11	-0.27	-70.8	81.2	0.90	0.33

surface POA emission (molecules/cm²/s)

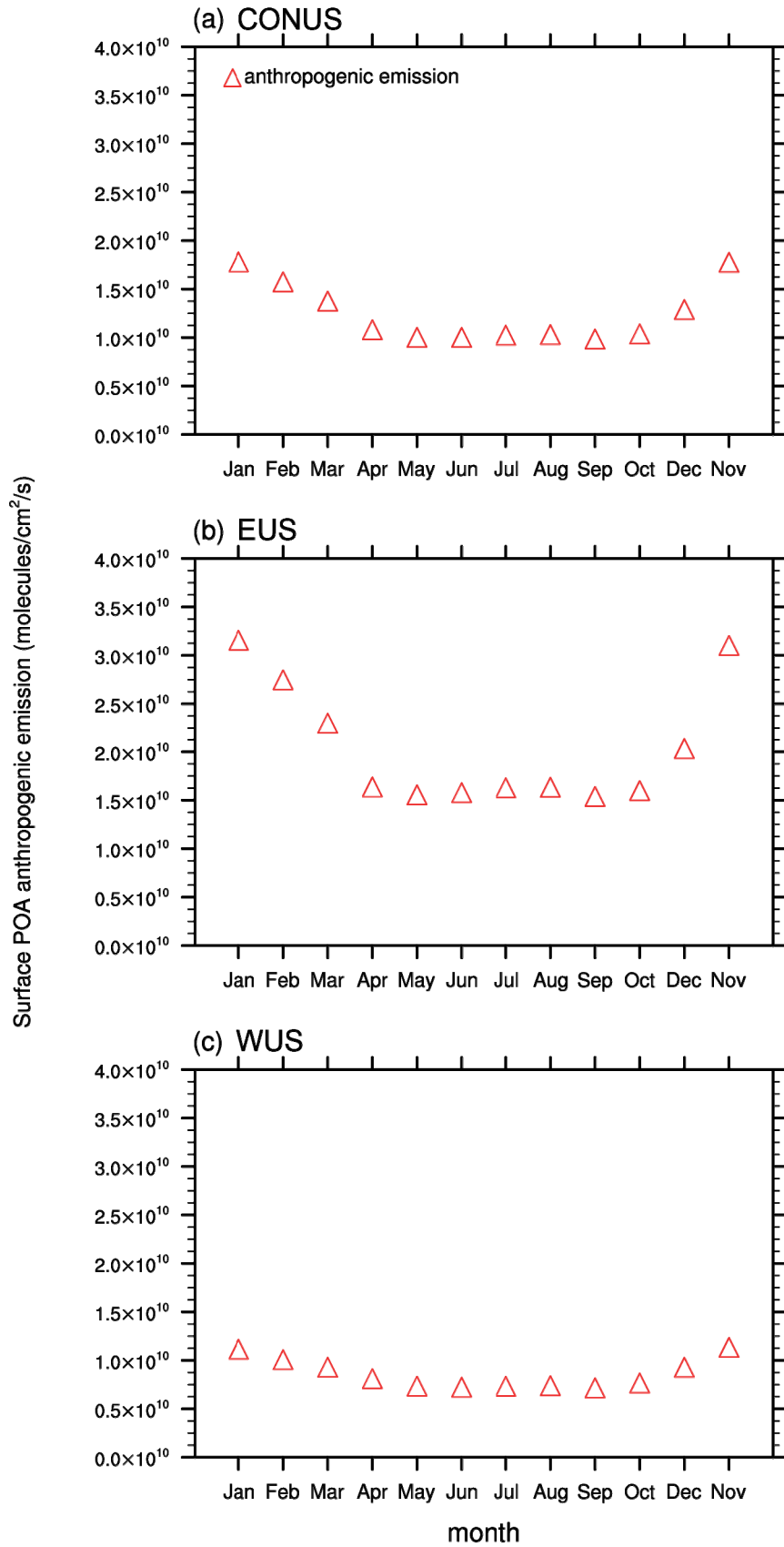


Figure. S1. seasonal cycle of 1988–2019 average surface Primary Organic Aerosol (POA) anthropogenic emission used for CAM-Chem-SD (red upper triangles) over CONUS (a), EUS (b) and WUS (c).

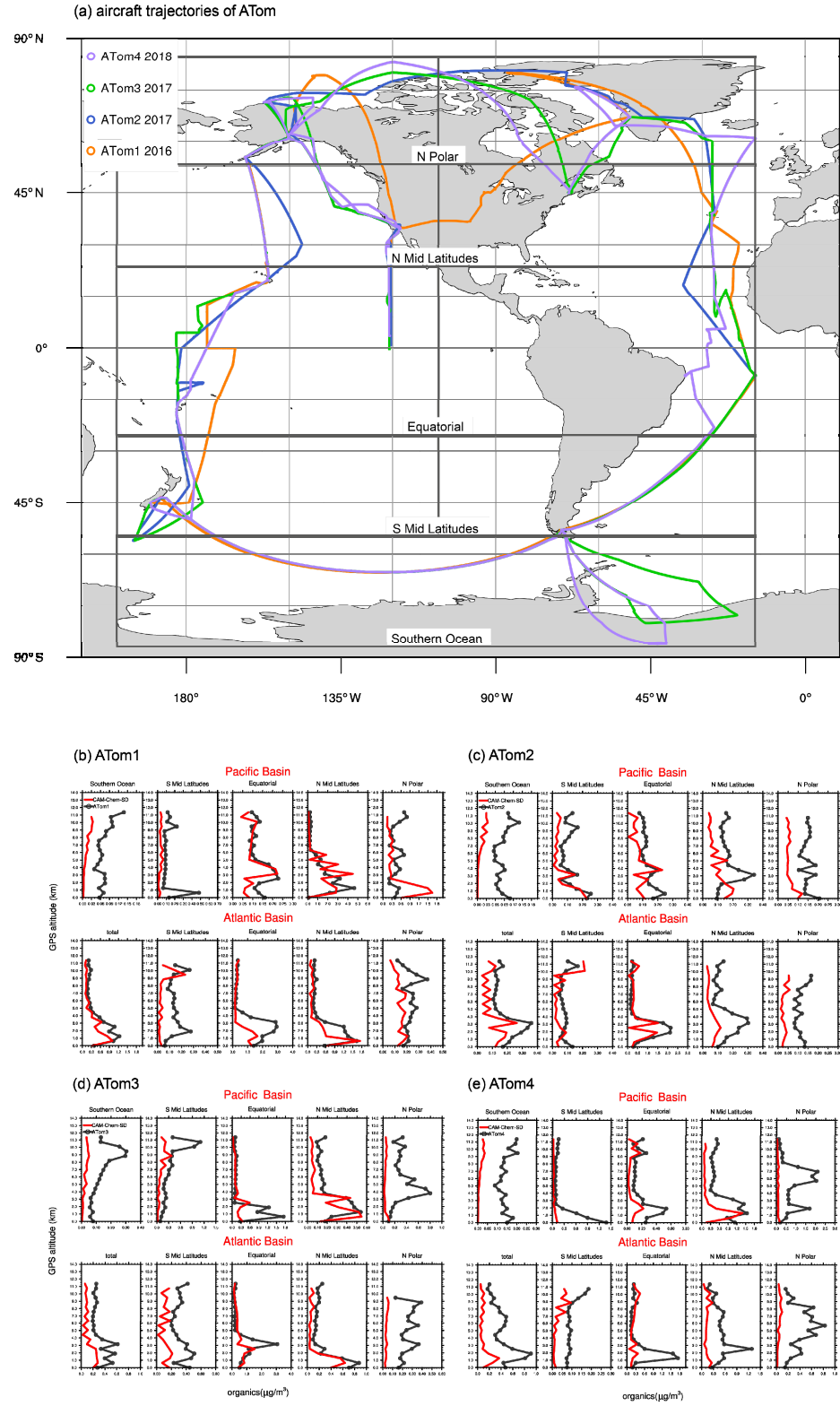


Figure. S2. Validation against ATom flight. (a) trajectories of four ATom flights; subdomains divisions are shown in grey boxes. Vertical profile of organics concentration of CAM-Chem-SD (red lines) and flight measurements (black marker lines) during ATom1 (b), ATom2 (c), ATom3 (d) and ATom4 (e) campaigns.

2010 July US average SOA concentration

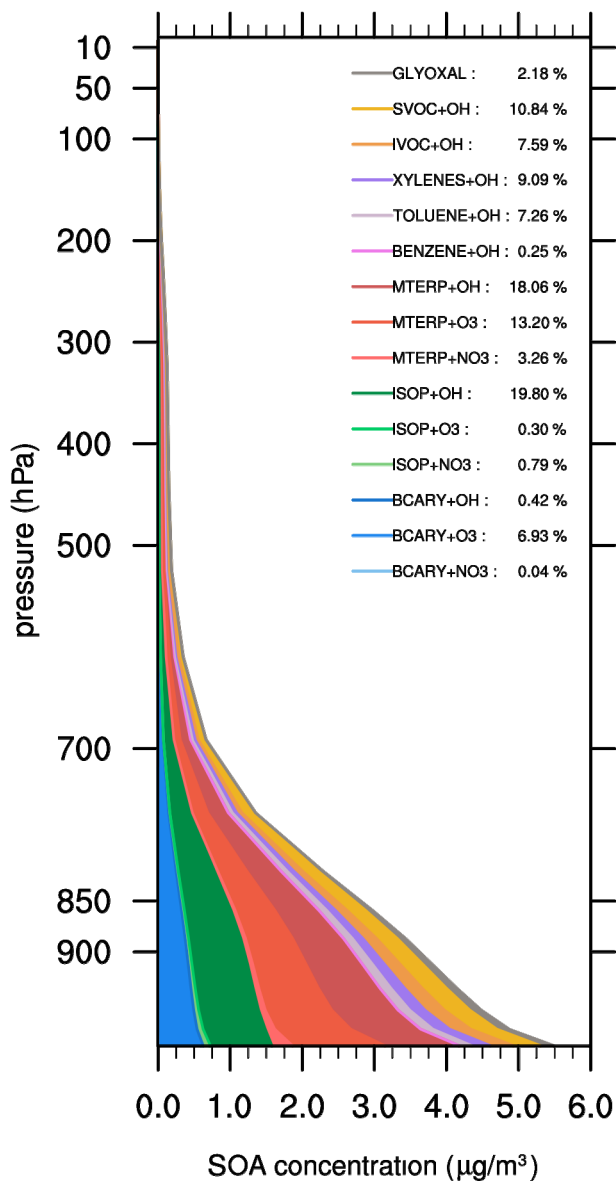


Figure. S3. Vertical profile of SOA formed by 15 reactions over US in July, 2010. The vertical average relative contribution of each reaction is shown as the number in the legend.

relationship between OA bias and VOCs flux of CAM-Chem-SD

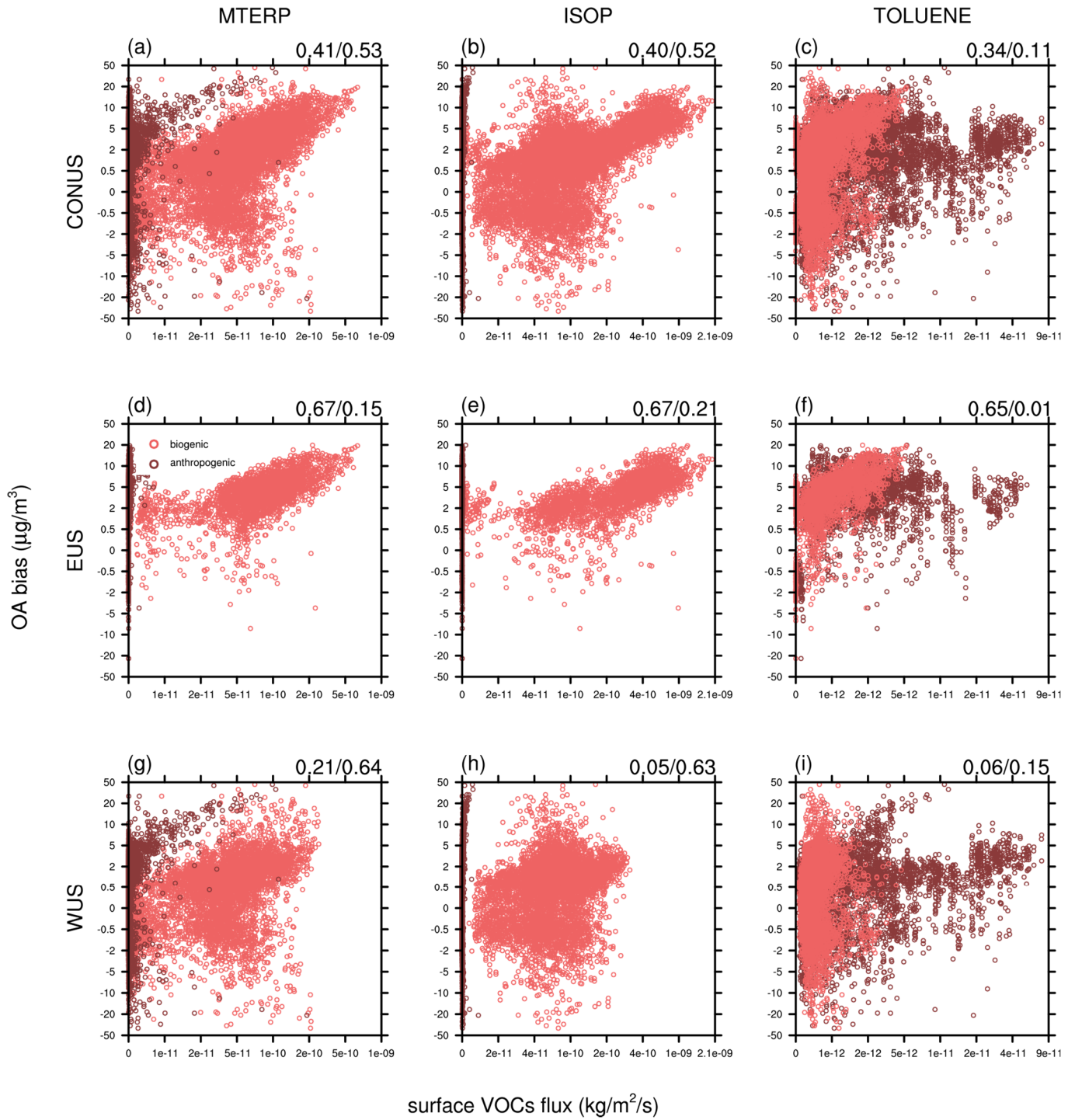


Figure. S4. The relationship between surface OA bias and MTERP (panel a, d, g), ISOP (panel b, e, h), TOLUENE (panel c, f, i) flux in the summer of 1988 to 2019 over CONUS (panel a ~ c), EUS (panel d ~ f) and WUS (panel g ~ i). Surface VOCs flux are split into biogenic emission flux from MEGAN (light red dots) and other flux referred as anthropogenic flux (dark red dots). The numbers shown in each panel are the correlation coefficient between OA bias and biogenic flux, followed by the correlation coefficient between OA bias and anthropogenic flux.

surface OA concentration ($\mu\text{g}/\text{m}^3$)

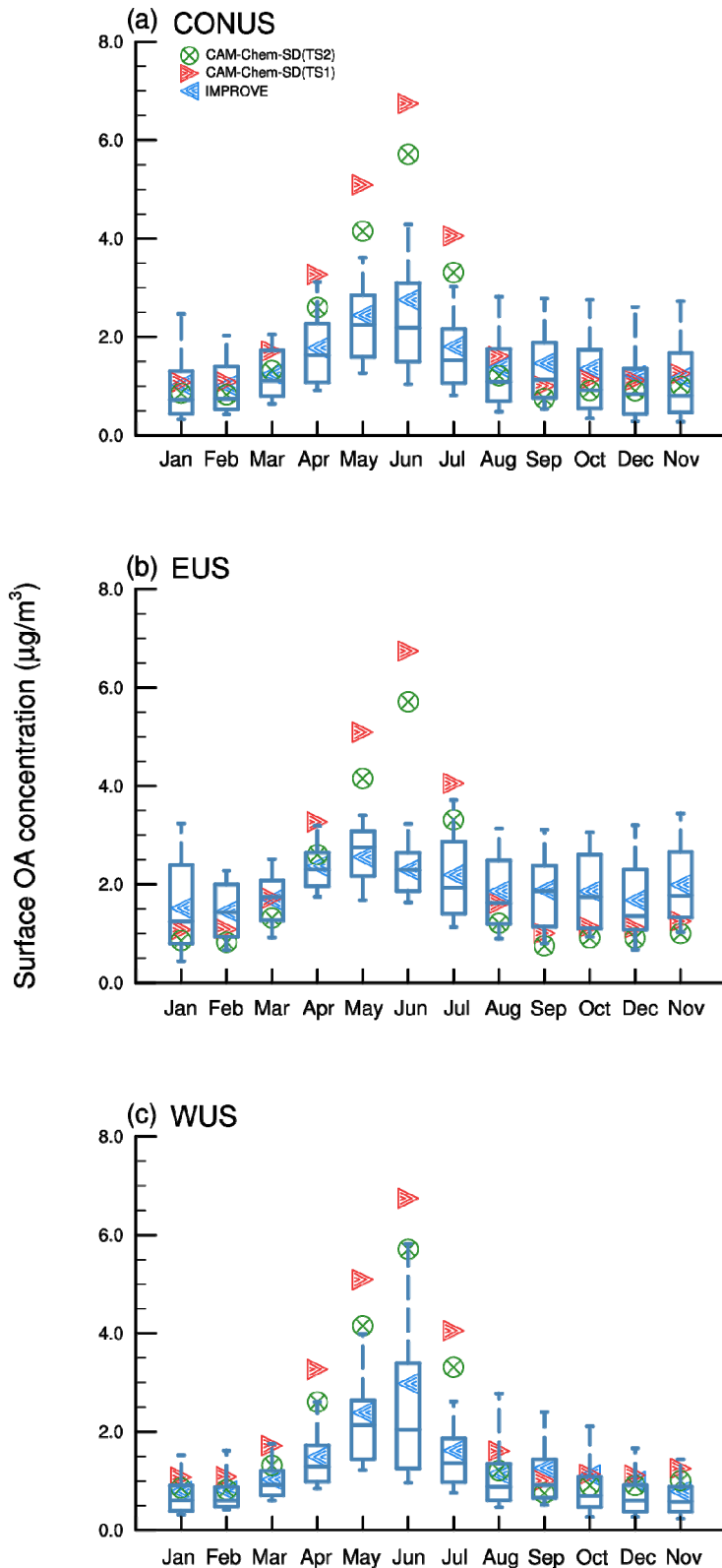


Figure. S5. 2013.03–2014.02 CONUS surface OA concentration of IMPROVE (blue dots), CAM-Chem-SD with MOZART-TS1 chemistry (red dots) and CAM-Chem-SD with MOZART-TS2 chemistry (green dots). Every blue box denotes the 10th, the 25th, the median, the 75th and the 90th percentiles of the observations for all selected sites in each month.

Reference:

Emmons, L. K., Schwantes, R. H., Orlando, J. J., Tyndall, G., Kinnison, D., Lamarque, J. F., Marsh, D., Mills, M. J., Tilmes, S., Bardeen, C., Buchholz, R. R., Conley, A., Gettelman, A., Garcia, R., Simpson, I., Blake, D. R., Meinardi, S., and Pétron, G.: The Chemistry Mechanism in the Community Earth System Model Version 2 (CESM2), *Journal of Advances in Modeling Earth Systems*, 12, 10.1029/2019ms001882, 2020.

Shrivastava, M., Easter, R. C., Liu, X., Zelenyuk, A., Singh, B., Zhang, K., Ma, P.-L., Chand, D., Ghan, S., Jimenez, J. L., Zhang, Q., Fast, J., Rasch, P. J., and Tiitta, P.: Global transformation and fate of SOA: Implications of low-volatility SOA and gas-phase fragmentation reactions, *Journal of Geophysical Research: Atmospheres*, 120, 4169–4195, 10.1002/2014jd022563, 2015.

Wofsy, S. C., Afshar, S., Allen, H. M., Apel, E. C., Asher, E. C., Barletta, B., Bent, J., Bian, H., Biggs, B. C., Blake, D. R., Blake, N., Bourgeois, I., Brock, C. A., Brune, W. H., Budney, J. W., Bui, T. P., Butler, A., Campuzano-Jost, P., Chang, C. S., Chin, M., Commane, R., Correa, G., Crounse, J. D., Cullis, P. D., Daube, B. C., Day, D. A., Dean-Day, J. M., Dibb, J. E., DiGangi, J. P., Diskin, G. S., Dollner, M., Elkins, J. W., Erdesz, F., Fiore, A. M., Flynn, C. M., Froyd, K. D., Gesler, D. W., Hall, S. R., Hanisco, T. F., Hannun, R. A., Hills, A. J., Hintsa, E. J., Hoffman, A., Hornbrook, R. S., Huey, L. G., Hughes, S., Jimenez, J. L., Johnson, B. J., Katich, J. M., Keeling, R. F., Kim, M. J., Kupc, A., Lait, L. R., Lamarque, J. F., Liu, J., McKain, K., McLaughlin, R. J., Meinardi, S., Miller, D. O., Montzka, S. A., Moore, F. L., Morgan, E. J., Murphy, D. M., Murray, L. T., Nault, B. A., Neuman, J. A., Newman, P. A., Nicely, J. M., Pan, X., Paplawsky, W., Peischl, J., Prather, M. J., Price, D. J., Ray, E. A., Reeves, J. M., Richardson, M., Rollins, A. W., Rosenlof, K. H., Ryerson, T. B., Scheuer, E., Schill, G. P., Schroder, J. C., Schwarz, J. P., St.Clair, J. M., Steenrod, S. D., Stephens, B. B., Strode, S. A., Sweeney, C., Tanner, D., Teng, A. P., Thames, A. B., Thompson, C. R., Ullmann, K., Veres, P. R., Vieznor, N., Wagner, N. L., Watt, A., Weber, R., Weinzierl, B., Wennberg, P. O., Williamson, C. J., Wilson, J. C., Wolfe, G. M., Woods, C. T., and Zeng, L. H.: ATom: Merged Atmospheric Chemistry, Trace Gases, and Aerosols, in, ORNL Distributed Active Archive Center, 2018.